

# Thickness evolution of coercivity in ultrathin magnetic films

R.A. Hyman<sup>1</sup>, A. Zangwill<sup>1</sup>, and M.D. Stiles<sup>2</sup>

<sup>1</sup>*School of Physics, Georgia Institute of Technology, Atlanta, GA 30332-0430*

<sup>2</sup>*Electron Physics Group, National Institute of Standards and Technology, Gaithersburg, MD 20899*

(June 18, 2021)

The thickness evolution of in-plane magnetization reversal in ultrathin films is studied with a theoretical model that takes account of surface roughness typical of epitaxial growth. Guided by Néel's model, step edge sites of monolayer-height islands are assigned a two-fold anisotropy in addition to a four-fold anisotropy at all sites. Coercivity is found to depend essentially on both the film thickness and the partial coverage of the topmost layer. Its qualitative features are determined primarily by sample geometry and the size of the step anisotropy compared to the domain wall energy. Magnetostatic interactions change the results quantitatively, but not qualitatively. Their effect is understood by comparing calculations with and without their inclusion.

PACS numbers: 75.70.-i,75.60.-d

The potential for novel physics and exciting applications has motivated many studies of ultrathin magnetic films [1]. To explore new physics, it is usual to focus on simple model systems and equilibrium properties such as exchange, anisotropy, and the thermodynamic phase diagram in the space of temperature and thickness. To exploit new applications, it is typical to study more complex systems and non-equilibrium properties such as hysteresis, domain wall motion, and magnetotransport. Common to both is the observation that variations in surface roughness and film morphology often have a significant effect on measurement results. This observation motivated the theoretical work reported below.

Magnetometry [2] and the surface magneto-optic Kerr effect (SMOKE) [3] are widely used to probe magnetization reversal and the origin of coercivity in ultrathin films. A typical experiment reports the coercive field as a function of total deposited material using a thickness scale calibrated in small fractions of a monolayer. While it is generally appreciated that the films in question exhibit surface roughness, the consequences of this fact are not often addressed explicitly. An exception is a theoretical argument presented a few years ago by Bruno *et al.* [4] Making simple assumptions regarding thickness fluctuations and the nature of domain wall pinning in films with *perpendicular* magnetization, he derived a coercive field  $H_C \propto t^{-5/2}$  where  $t$  is the film thickness. Experimental tests of this prediction for the Co/Pd(111) [5] and Co/Pt(111) [6] systems have yielded contradictory results.

In this paper, we study hysteresis and coercivity as a function of thickness for a model ultrathin film with *in-plane* magnetization and surface roughness typical of

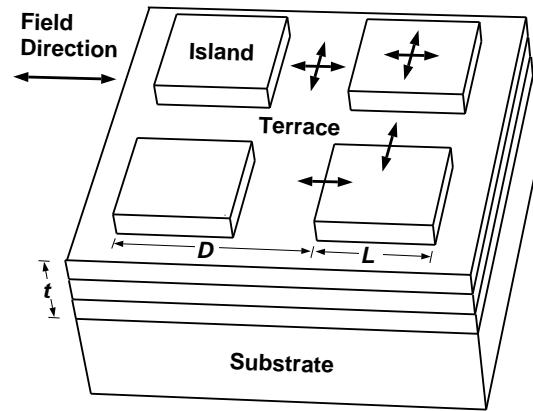


FIG. 1. Schematic view of the rough ultrathin film morphology used in this work. The indicated island geometry is repeated periodically. Arrows indicate local anisotropy axes for  $K_4 > 0$  and  $K_2 < 0$ .

as-grown samples. No universal law is found. Instead, the coercive field is found to depend on both the film thickness and the partial coverage of the topmost incomplete layer. Our conclusion is based on zero-temperature numerical simulations of magnetization reversal using a generalization of a classical spin model of an ultrathin film introduced previously [7].

The model cubic film (Figure 1) sits atop a non-magnetic substrate and takes the form of a periodic array of square, monolayer-height, magnetic islands of side length  $L$  and center-to-center separation  $D$  arranged on top of  $1 \leq t \leq 5$  complete magnetic layers. To model centered cubic lattices, the variable  $t$  is measured in units of  $t_0 = a/2$  where  $a$  is the in-plane lattice constant. Classical Heisenberg spins at each surface site  $i$  point in the direction  $\hat{S}_i$ . At each site in the surface, the spins are locked throughout the thickness of the film giving a two-dimensional model. This two-dimensional model is appropriate if the film thickness is much less than the exchange length. Each spin is subject to nearest-

neighbor ferromagnetic exchange  $J$ , an out-of plane surface anisotropy  $K_Z > 0$ , a four-fold in-plane anisotropy  $K_4 > 0$ , Zeeman energy from an external field  $H$ , and a two-fold anisotropy  $K_2$  at island perimeter sites only. A Néel model analysis [8] shows that the latter arises because step edges break translational symmetry in the surface plane. We also take account of the fact that spins at step edges experience reduced exchange compared to spins elsewhere on an island.

The magnetic energy is

$$\begin{aligned}
E_M = & - \sum_{\langle i,j \rangle} J_{ij} \hat{\mathbf{S}}_i \cdot \hat{\mathbf{S}}_j - a^2 K_2 \sum_{i \in \text{step}} (\hat{\mathbf{S}}_i \cdot \hat{\mathbf{b}}_i)^2 \\
& - 2a^2 K_4 \sum_i t_i [(\hat{S}_i^x)^4 + (\hat{S}_i^y)^4] - \mu \mathbf{H} \cdot \sum_i t_i \hat{\mathbf{S}}_i \\
& + a^2 K_Z \sum_i (\hat{S}_i^z)^2
\end{aligned} \quad (1)$$

where  $t_i$  is the film height at site  $i$  in units of  $t_0$ ,  $\hat{\mathbf{b}}_i$  is a unit vector parallel to the local step edge,  $J_{ij} = J \min[t_i, t_j]$ , and  $\mu = \mu_0 a^2 t_0 M_S$  where  $\mu_0$  is the magnetic permeability in SI units and  $M_S$  is the saturation magnetization. Note that, although  $K_2 > 0$  corresponds to an anisotropy axis parallel ( $K_2 > 0$  would be perpendicular) to the step edge, for the highly symmetrical island geometry studied here the energy (1) is invariant to a change in the sign of  $K_2$  and a simultaneous rotation of the external field and all spins by  $90^\circ$  in plane. Thus, the same reversal dynamics is expected for both signs of  $K_2$ . Typical values of the material parameters,  $J \sim 10^{-21}$  J and  $K_4 \sim 1 \times 10^{-3}$  mJ/m<sup>2</sup> (1 mJ/m<sup>2</sup>=1 erg/cm<sup>2</sup>), [9] imply a domain wall width  $W \simeq 8\sqrt{J/2K_4} \simeq 600a$ . The numerical results reported below all use the values  $|K_2| = K_Z \sim 1$  mJ/m<sup>2</sup> [2],  $a = 0.3$  nm, and  $\mu \sim 2 \times 10^{-23}$  J/T in addition to those quoted above for  $J$  and  $K_4$ . The lengths  $L$  and  $D$  are measured in spin block units of  $10a \sim W/60$ , a distance over which no appreciable spin rotation occurs.

Beginning with a large positive value of  $\mathbf{H} = H \hat{x} \parallel [100]$ , the local minimum of (1) was followed as the field was reversed adiabatically by a combination of conjugate gradient minimization and relaxational spin dynamics [7]. The solid curves in Figure 2 illustrate the variation of the computed coercive field  $H_C$  with coverage  $\Theta = L^2/D^2$  when the incomplete magnetic layer sits atop  $t=1, 3, 5$  complete magnetic layers. Note that  $H_C$  is normalized to the Stoner-Wohlfarth value  $H_{SW} = 8a^2 K_4/\mu$  where easy-axis reversal occurs for a single domain system with four-fold anisotropy [10]. Because  $K_Z$  is large enough to keep the spins in plane, the  $t=1$  curve agrees with our previous XY-model results [7]. They also agree semi-quantitatively with SMOKE data reported by Buckley *et al.* [11] for the Cu/Co/Cu(001) system. The rather different  $t=3$  and  $t=5$  results can only reflect the decreasing importance of the surface anisotropy, which scales like  $K_2^* = K_2/t$  relative to other terms in the magnetic energy. It is apparent from Figure 2 that the coer-

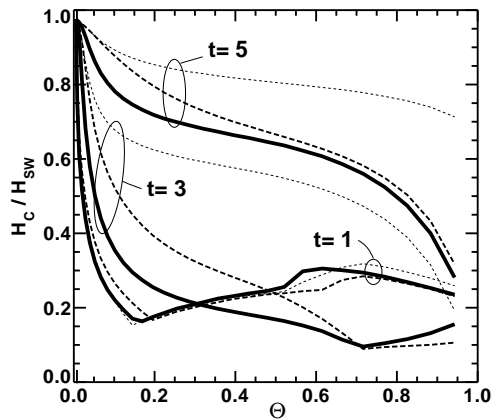


FIG. 2. Scaled coercive field as a function of  $L/D$  when the incomplete magnetic layer sits on  $t = 1, 3, 5$  complete magnetic layers.  $D = 64$ . The solid curves give the results without magnetostatics. The heavy dashed curve and light dashed curve give the results with magnetostatics for the cases of step anisotropy parallel and perpendicular to the steps respectively.

civity depends not only on film thickness but also on the partial coverage of the topmost incomplete layer. The reasons for this are best understood by study of the corresponding magnetization curves.

The hysteresis loops calculated during adiabatic cycling of the field for  $t=1, 3, 5$  and relatively *large* islands ( $\Theta \simeq \frac{3}{4}$ ) are shown in Figure 3. The  $t=1$  reversal scenario is understood [7,12]. Reversal initiates at those step edges where the anisotropy axis is along the  $y$  axis, (perpendicular to the saturated state spin direction) because spins at those sites experience the greatest torque. This first deviation from the positive saturated state occurs at  $H = H_N > 0$ , the nucleation field. The rotated spins form small lens-shaped domains pinned at the island edges within which, near  $H = 0$ , the spins are oriented nearly  $90^\circ$  to the original saturation direction. The domain walls depin from the steps at the island edges at a (negative) field  $|H| = H_S \sim (W/L)H_{SW}$  [13] and the magnetization jumps to a configuration where the  $90^\circ$  state covers the islands except near the complementary step edges where the anisotropy axis is along the  $x$  axis, i.e., where the two-fold axis locally pins the spins parallel to the saturated state spin direction. Coherent rotation of the island spins occurs as the external field is made more negative (the coercive field occurs in this interval)

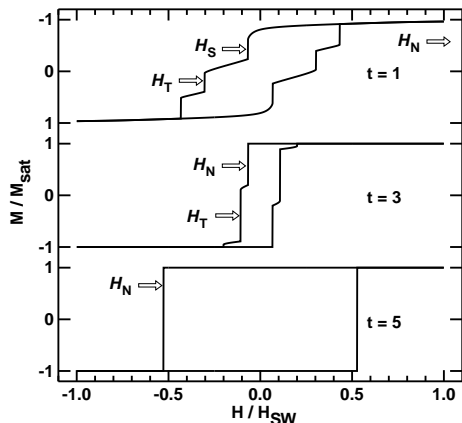


FIG. 3. Calculated film magnetization projected onto  $\mathbf{H} \parallel \hat{x}$  for films of thickness  $t = 1, 3, 5$  and large islands with  $L = 56$  and  $D = 64$ .

until at  $|H| = H_T$  [13], another magnetization jump occurs when the  $90^\circ$  single-domain state on the island terraces suffers a Stoner-Wohlfarth instability to complete reversal (the  $180^\circ$  state). A final jump occurs when the external field induces the complementary step-edge spins to flip from  $0^\circ$  to  $180^\circ$  and the reversal is complete.

The  $t=3$  loop in Figure 3 differs from the  $t=1$  loop in three important ways: (1) the nucleation field is negative rather than positive and coincides with a jump in magnetization; (2) the coercive field is smaller; and (3) there are two magnetization jumps rather than three. Since nucleation occurs at two parallel step edges per island, the origin of the change in sign of  $H_N$  can be understood from the authors' recent analysis of magnetic reversal on vicinal surfaces [14]. We showed there that, for a single step (infinitely separated from other steps) on an otherwise flat ultrathin magnetic film, reversal nucleates at  $H_N^\infty = H_{SW}(\mathcal{K}^2 - 1)$  where  $\mathcal{K} = aK_2^*/2\sqrt{2JK_4}$  is a dimensionless measure of the effective step anisotropy. Since  $\mathcal{K} \sim 1$  for realistic values of the magnetic parameters (as used here), it is not surprising that  $H_N$  can change from positive to negative as the value of  $K_2^*$  decreases. In fact,  $|H_N| > H_S$  in this instance, so nucleation is accompanied by an immediate jump to the  $90^\circ$  state on the islands.

Coherent rotation begins when the external field is made more negative as in the  $t=1$  case but the rotation is abruptly cut off here by a jump of the island terrace spins to the  $180^\circ$  reversed state. The corresponding jump oc-

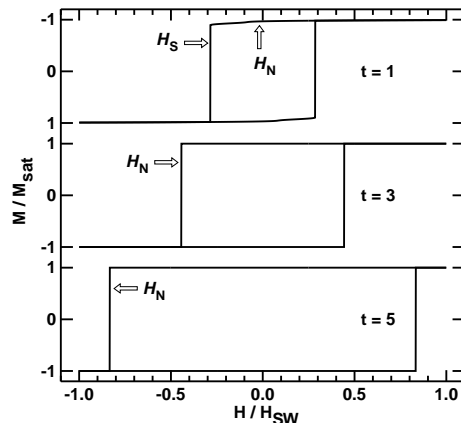


FIG. 4. Calculated film magnetization projected onto  $\mathbf{H} \parallel \hat{x}$  for films of thickness  $t = 1, 3, 5$  and small islands with  $L = 16$  and  $D = 64$ .

curred at a much larger (negative) value of external field for the  $t=1$  film. This occurs because rotation of island terrace spins away from the  $90^\circ$  state costs exchange energy near every island edge due to the two-fold anisotropy at each step. The reduction in  $H_T$  seen in Figure 3 from  $t=1$  to  $t=3$  is thus expected because the effective two-fold anisotropy is reduced for thicker films. It happens that  $H_C = H_T$  in this case. Only a coherent rotation of the complementary step spins is required to complete reversal now because  $K_2^*$  is here too small to strongly pin those spins in the original saturation direction.

The  $t=5$  hysteresis loop in Figure 3 is easily explained because the formula quoted above for  $H_N^\infty$  predicts an even larger value for the nucleation field as  $\tilde{K}_2$  continues to decrease. A simple square loop is found because  $|H_N|$  is greater than both  $H_S$  and  $H_T$ .  $H_C = H_N$  and the entire film acts as a single domain particle.

Figure 4 is the same as Figure 3 except that the magnetization curves are shown for relatively *small* islands ( $\Theta \simeq 1/16$ ). The  $t=1$  loop evidently differs drastically from the corresponding loop for large islands. The nucleation field  $H_N > 0$  but the much smaller island size ( $L$ ) drives the value of  $H_S \sim (W/L)H_{SW}$  so large that it exceeds  $H_T$ . A direct jump to nearly complete reversal occurs at  $H_C = H_S$ . The change in sign of  $H_N$  explained above occurs between  $t=1$  and  $t=3$  as before. But now the sequence  $|H_N| > H_S > H_T$  guarantees that only a square loop will be found for  $t=3$  in Figure 4. The approach of  $H_C = H_N$  to  $H_{SW}$  observed for the  $t=5$  loop

follows from the same argument based on  $H_N^\infty$  as was advanced earlier for the large island case.

Since  $H_C = H_N$  for  $t \geq 5$ , the  $t=5$  solid curve for  $H_C$  in Figure 2 actually shows the island size dependence of  $H_N$ . The results are comparable to the nucleation field dependence on step separation for a periodic array of steps separated by a finite distance [14]. Those results, presented in Figure 7 of Ref. [14], show  $H_N$  rapidly approaching zero (from negative values) as the step spacing decreases through values comparable to the distance between adjacent steps used in the present work. Qualitatively, nucleation is easier when steps are close together because the intervening spins tend to rotate also and thus reduce the total exchange energy cost.

It has been argued that magnetostatics has a negligible effect on the hysteresis of ultrathin films with in-plane magnetization [15]. We checked this explicitly by adding a dipole-dipole energy term to the magnetic energy (1). In the continuum limit, this term can be written

$$E_D = -\frac{\mu_0}{2} \int d\mathbf{r} \mathbf{M} \cdot \mathbf{H}_D \quad (2)$$

where the dipolar field  $\mathbf{H}_D$  is found by solving the Maxwell equations  $\nabla \cdot \mathbf{H}_D = -\nabla \cdot \mathbf{M}$  and  $\nabla \times \mathbf{H}_D = 0$ . In practice, these equations are discretized and  $\mathbf{M}_i = M_S \hat{\mathbf{S}}_i$  throughout the thickness of the film at site  $i$ . In a system without step edges any form of magnetization inhomogeneity is disfavored by magnetostatics because the uniform state absolutely minimizes the dipolar energy. In systems with step edges spin alignment parallel to steps is favored to avoid exposed magnetic poles. This breaks the symmetry noted earlier regarding the sign of  $K_2$ . Roughly speaking, magnetostatics tends to enhance the step anisotropy when  $K_2 < 0$  (easy axis parallel to the steps) and weaken the step anisotropy when  $K_2 > 0$  (easy axis perpendicular to the steps). We examined both cases.

The computational methodology used by us to evaluate the dipole energy is similar to that described by Mansuripur [16]. The curves with short (long) dashes in Figure 2 represent the coercive field including magnetostatics for the case of  $K_2 > 0$  ( $K_2 < 0$ ). Practically no effect is seen for  $t=1$  as suggested in Ref. [15]. But the  $t=5$  curves show just the combination of effects expected qualitatively. Nucleation at steps unavoidably generates magnetization inhomogeneities so a larger driving force ( $H_N$ ) is required to initiate reversal. This effect is partly compensated when  $K_2 < 0$  when the intrinsic step anisotropy is parallel to the step. Conversely, nucleation is even more retarded when magnetostatics works to further reduce  $K_2^*$ .

When  $H_C$  is determined by nucleation (all of the  $t=5$  curve and  $t=3$  up to about  $\Theta = 3/4$ ), the systematics of the magnetostatic results can be understood by noting that the source of magnetostatic energy is  $\nabla \cdot \mathbf{M} = \partial_x M_x + \partial_y M_y$ . At saturation,  $M_x$  is a constant and  $M_y = 0$ . To lowest order,  $M_x$  remains constant at

nucleation so only the variations of  $M_y$  in the  $y$  direction contribute to  $E_D$ . We have seen that the magnetization pattern at nucleation consists of lens-shaped domains centered on those step edges where the local anisotropy axis points in the  $y$  direction [17]. At the smallest coverages when the islands are very small,  $M_y = M_y(x, y)$  is a function of both  $x$  and  $y$  so a finite magnetostatic effect is expected. This effect increases as the island size increases initially because more step edge contributes to nucleation. But for large enough island size, the magnetization pattern at nucleation more nearly resembles the vicinal surface case [14] and  $M_y = M_y(y)$  when  $K_2 < 0$  and  $M_y = M_y(x)$  when  $K_2 > 0$ . The effect of magnetostatics thus increases in the former case and disappears in the latter case as the islands grow larger. This is the trend seen in Figure 2 except for the very highest coverages of  $t=3$  when  $H_C$  is not determined by nucleation [7,12].

Note also that magnetostatics has a weaker effect for  $t=5$  than for  $t=3$ . This is so because the thicker film experiences a relatively weaker step anisotropy and behaves like a Stoner-Wohlfarth particle. The magnetization is more uniform and  $\nabla \cdot \mathbf{M}$  and  $E_D$  are reduced accordingly.

In summary, we have used a classical spin model to study zero temperature, in-plane, magnetization reversal in ultrathin films with surface roughness characteristic of the epitaxial growth process. The model includes four-fold anisotropy at all sites, two-fold anisotropy at step edge sites, and magnetostatic interactions. The coercive field was found to vary non-monotonically (but explicable) as a function of both film thickness and the partial coverage of the surface layer. We conclude that measurements of the thickness dependence of the coercive field and related hysteretic properties of ultrathin films with in-plane magnetization should not be expected to exhibit universal behavior. The results can depend sensitively on the film morphology which, in turn, can depend sensitively on growth conditions. Comparisons of nominally identical measurements on nominally identical systems in ignorance of the film morphology is unwarranted and can be seriously misleading.

R. A. H. acknowledges support from National Science Foundation Grant No. DMR-9531115. M. D. S. acknowledges useful conversations with R. D. McMichael.

- 
- [1] *Ultrathin Magnetic Structures I*, edited by J.A.C. Bland and B. Heinrich (Springer-Verlag, Berlin, 1994) and *Ultrathin Magnetic Structures II*, edited by B. Heinrich and J. A. C. Bland (Springer-Verlag, Berlin, 1994)
  - [2] U. Gradmann, in *Handbook of Magnetic Materials*, Volume 7, edited by K.H.J. Buschow (Elsevier, 1993), Chapter 1.

- [3] S. D. Bader and J. L. Erskine, in Ref. [1].
- [4] P. Bruno, G. Bayreuther, P. Beauvillain, C. Chappert, G. Lugert, D. Renard, J. P. Renard, and J. Seiden, *J. Appl. Phys.* **68**, 5759 (1990).
- [5] S. T. Purcell, M. T. Johnson, N. W. E. McGee, J. J. de Vries, W. B. Zeper, and W. Hoving, *J. Appl. Phys.* **73**, 1360 (1993); T. Kingetsu, *Jpn. J. Appl. Phys.* **33**, 1890 (1994).
- [6] N. W. E. McGee, M. T. Johnson, J. J. de Vries, and J. aan de Stegge, *J. Appl. Phys.* **73**, 3418 (1993); T. Kingetsu, *Jpn. J. Appl. Phys. Part 2* **33**, L1406 (1994).
- [7] A. Moschel, R. A. Hyman, A. Zangwill, and M. D. Stiles, *Phys. Rev. Lett.* **77**, 3653 (1996).
- [8] M. Albrecht, T. Furubayashi, M. Przybylski, J. Korcki, and U. Gradmann, *J. Mag. Mag. Mat.* **113**, 207 (1992).
- [9] B. Heinrich and J. F. Cochran, *Adv. Phys.* **42**, 523 (1993). These are the values used in Refs. [7,12]. The size of the four-fold anisotropy was misstated there as  $K_4 \sim 1 \times 10^{-2} \text{mJ/m}^2$ .
- [10] E. C. Stoner and E. P. Wohlfarth, *Phil. Trans. Roy. Soc. A* **240**, 74 (1948).
- [11] M. E. Buckley, F. O. Schumann, and J. A. C. Bland, *Phys. Rev. B* **52**, 6596 (1995); M. E. Buckley, F. O. Schumann, and J. A. C. Bland, *J. Phys. Cond. Matt.* **8**, L147 (1996).
- [12] R. A. Hyman, M. D. Stiles, L.-H. Tang, and A. Zangwill, *J. Appl. Phys.* **81**, 3911 (1997).
- [13] The symbols  $H_S$  and  $H_T$  are used to remind the reader that the corresponding magnetization jumps are initiated by spins on the islands steps and terraces, respectively. This usage conforms to the notation used in Ref. [14]. The less descriptive symbols  $H_L$  and  $H_{\perp}$  were used in Ref. [7] and Ref. [12].
- [14] R. A. Hyman, A. Zangwill, M. D. Stiles, *Magnetic Reversal on Vicinal Surfaces*, cond-mat/9804009, (accepted for publication in *Phys. Rev. B*).
- [15] A. S. Arrott, *J. Appl. Phys.* **69**, 5212 (1991); A. S. Arrott and B. Heinrich, *J. Magn. Magn. Mater.* **93**, 571 (1991).
- [16] M. Mansuripur, *The Physical Principles of Magneto-optical Recording* (Cambridge University Press, Cambridge, 1995), Section 13.2.
- [17] The magnetization pattern at nucleation discussed here is unstable if a jump in magnetization accompanies nucleation. But this pattern is still used to determine the energy barrier to nucleation. See Ref. [14] for more details.